

Supporting Information

Dithiolato- and halogenido-bridged nickel-iron complexes related to the active site of [NiFe]-H₂ases: preparation, structures, and electrocatalytic H₂ production

Li-Cheng Song,^{*a,b} Xiao-Feng Han,^a Wei Chen,^a Jia-Peng Li,^a
and Xu-Yong Wang^a

^aDepartment of Chemistry, State Key Laboratory of Elemento-Organic Chemistry, College of Chemistry and ^bCollaborative Innovation Center of Chemical Science and Engineering (Tianjin), Nankai University, Tianjin 300071, China

Contents:

1. IR and ¹H (³¹P) NMR spectra of 3a (Fig. S1–S3)
2. IR and ¹H (³¹P) NMR spectra of 4b (Fig. S4–S6)
3. Molecular structure of 3b and 4b (Fig. S7 and S8)
4. IR and ¹H (³¹P, ¹¹B, ¹⁹F) NMR spectra of 5b (Fig. S9–S13)
5. IR and ¹H (³¹P, ¹¹B, ¹⁹F) NMR spectra of 6a (Fig. S14–S18)
6. IR and ¹H (³¹P, ¹¹B, ¹⁹F) NMR spectra of 7a (Fig. S19–S23)
7. Bulk electrolysis for the two-electron reduction of [CpFe(CO)₂]₂ and the one-electron reductions of 5a–7a (Fig. S24)
8. Bulk electrolysis for the two-electron reduction of [CpFe(CO)₂]₂ and the one-electron oxidations of 5a–7a (Fig. S25)
9. Plots of *i*_p versus *v*^{1/2} for the reduction peaks of 5a–7a (Fig. S26)
10. Cyclic voltammograms and overpotential determinations of 6a,b, 7a,b with Cl₂CHCO₂H in MeCN (Fig. S27)
11. TOF calculations
12. References

1. IR and ^1H (^{31}P) NMR spectra of 3a

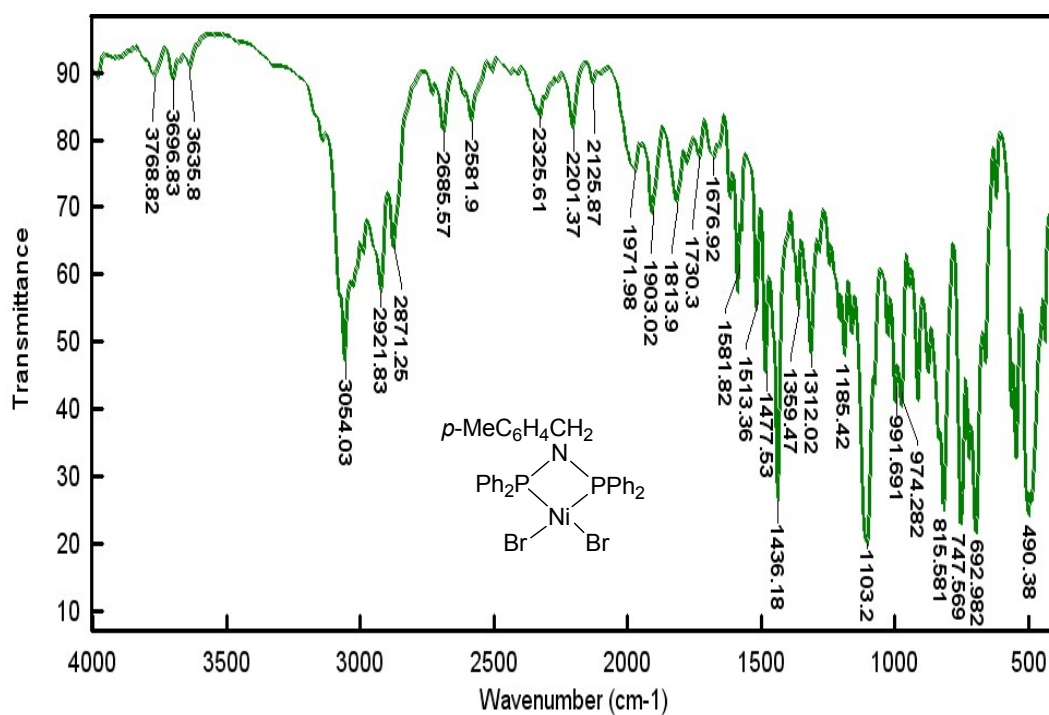


Fig. S1 IR spectrum of 3a.

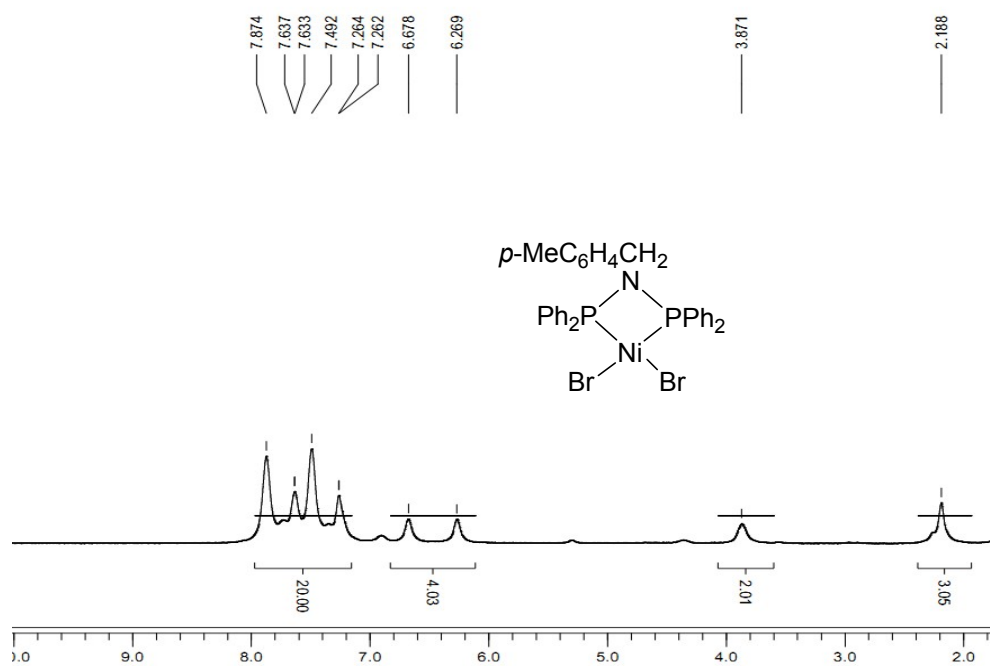


Fig. S2 ^1H NMR spectrum of 3a.

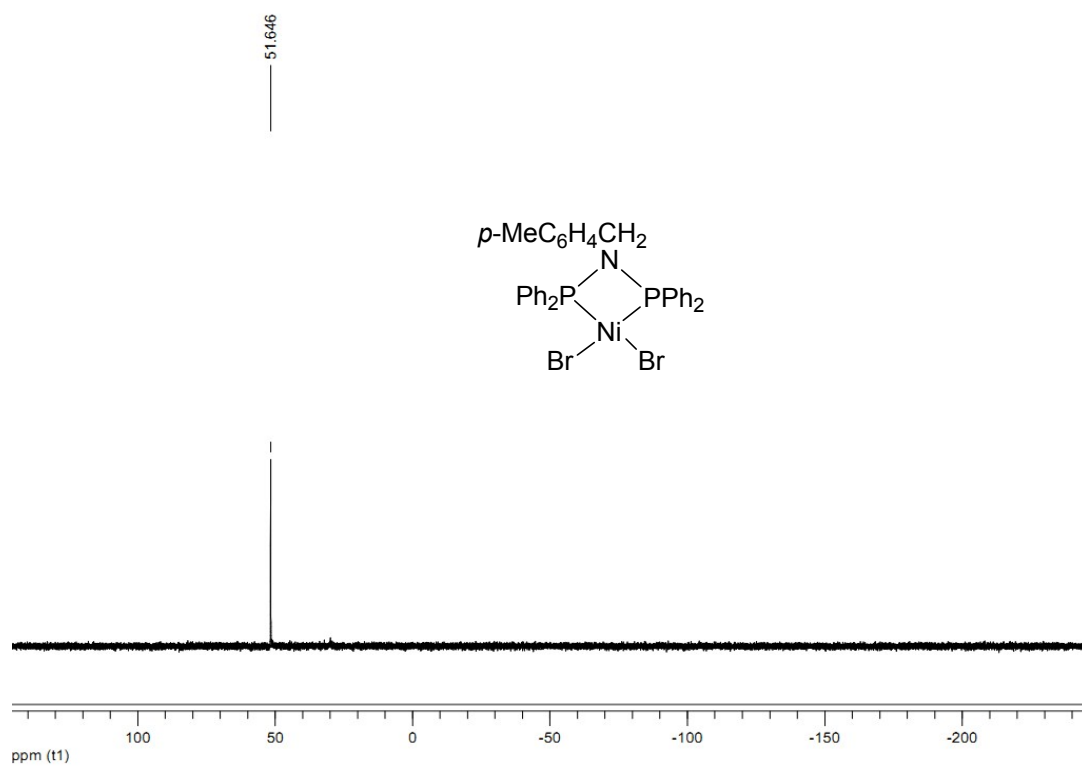


Fig. S3 ^{31}P NMR spectrum of **3a**.

2. IR and ^1H (^{31}P) NMR spectra of **4b**

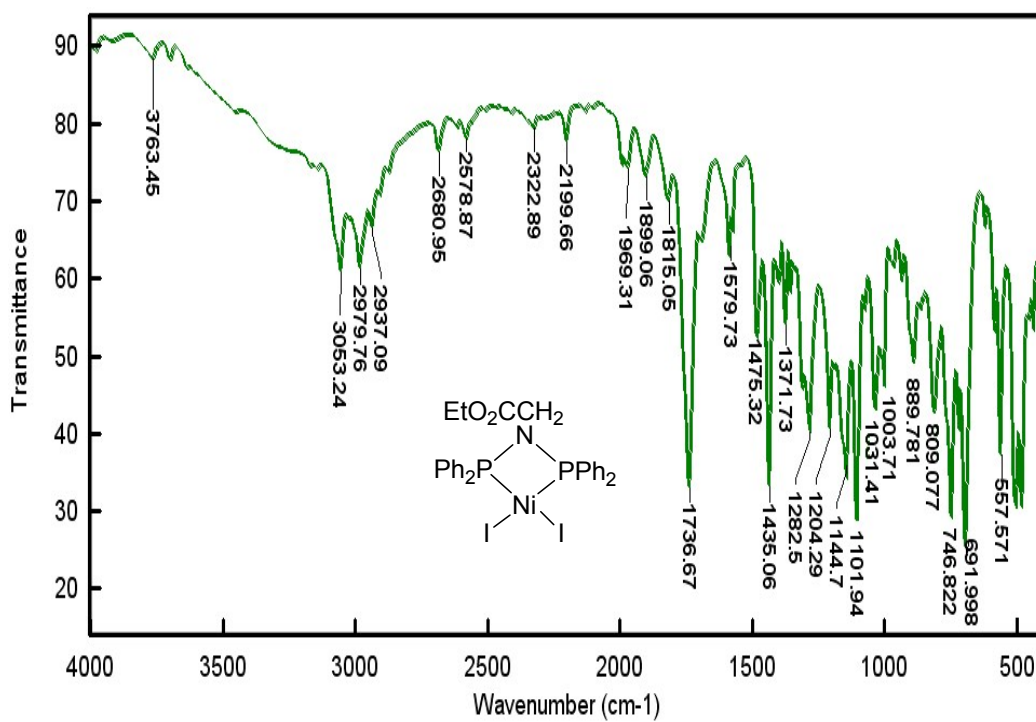


Fig. S4 IR spectrum of **4b**.

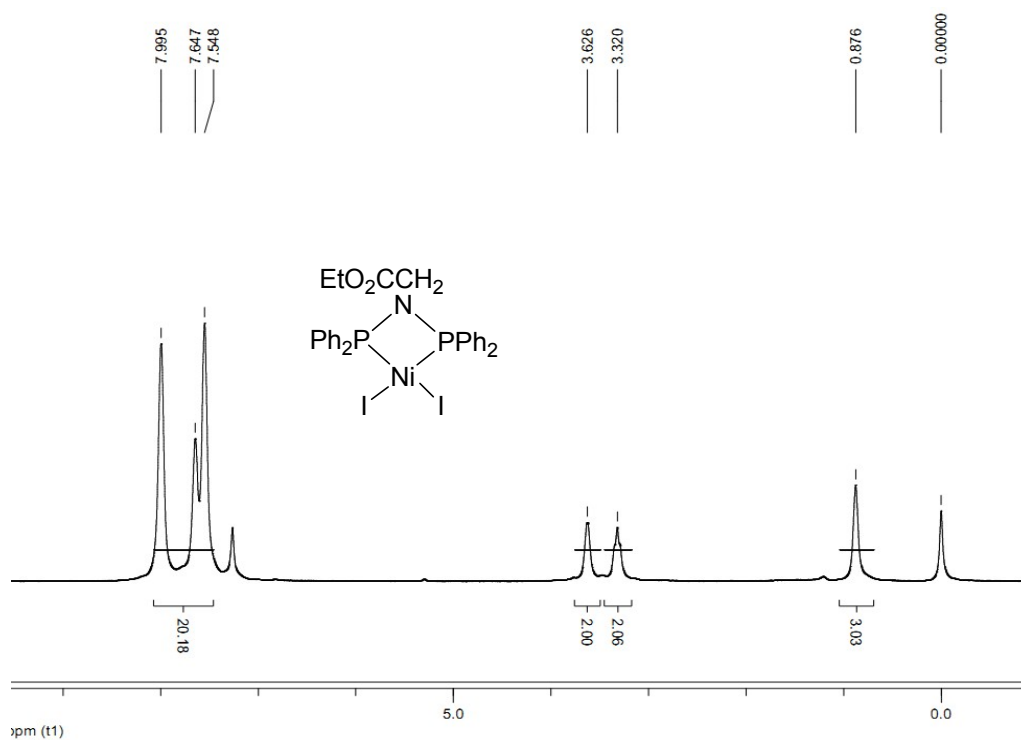


Fig. S5 ^1H NMR spectrum of **4b**.

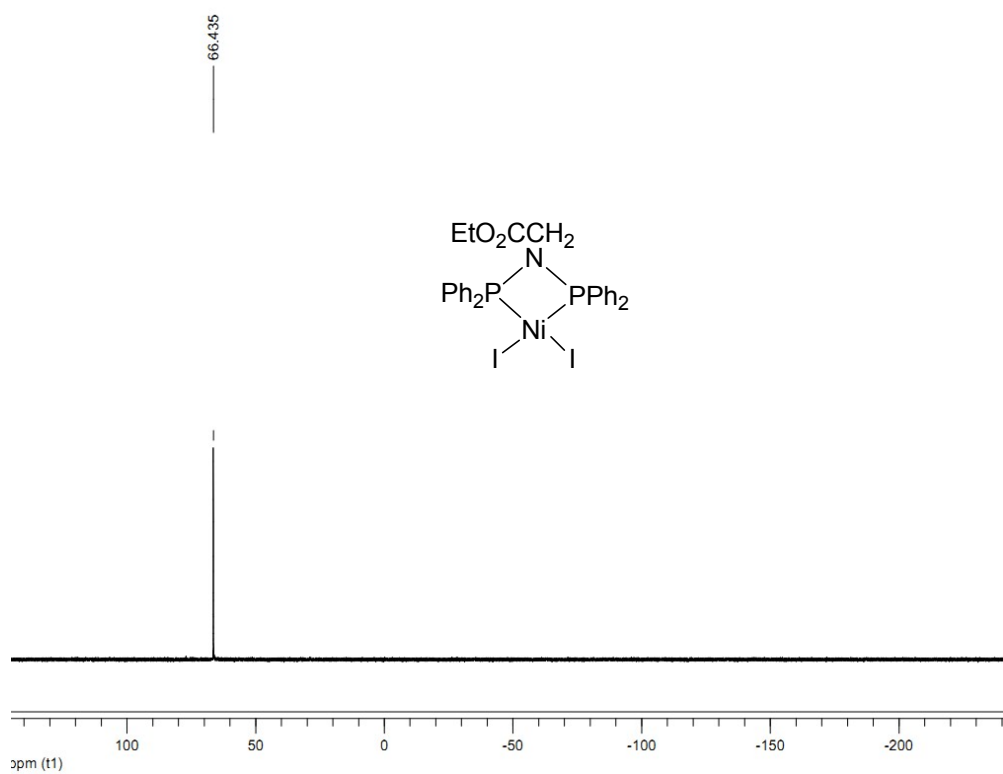


Fig. S6 ^{31}P NMR spectrum of **4b**.

3. Molecular structure of 3b and 4b.

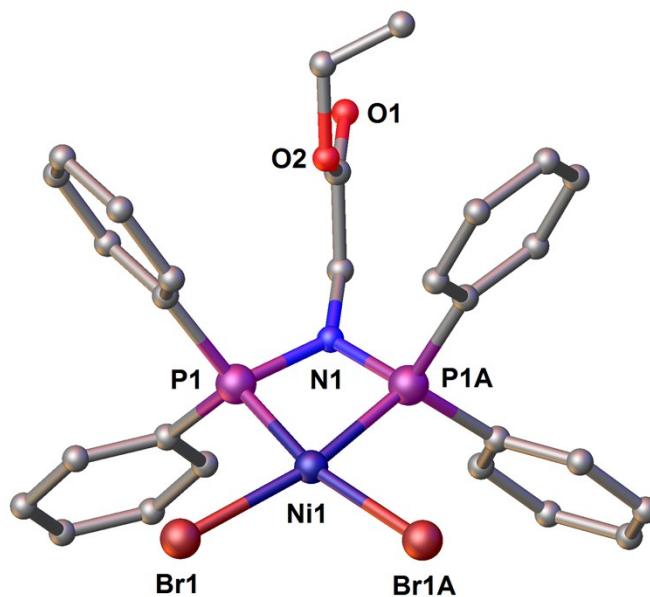


Fig. S7 Molecular structure of **3b**. Hydrogen atoms are omitted for clarity. Selected interatomic distances (Å) and angles (°) : Ni1–P1 2.1257 (8), Ni1–Br1 2.3393(5), P1–N1 1.698(2); P1–Ni1–P1A 73.75(4), P1–Ni1–Br1 93.23(2), Br1–Ni1–Br1A 99.80(3), P1–N1–P1A 97.36(17).

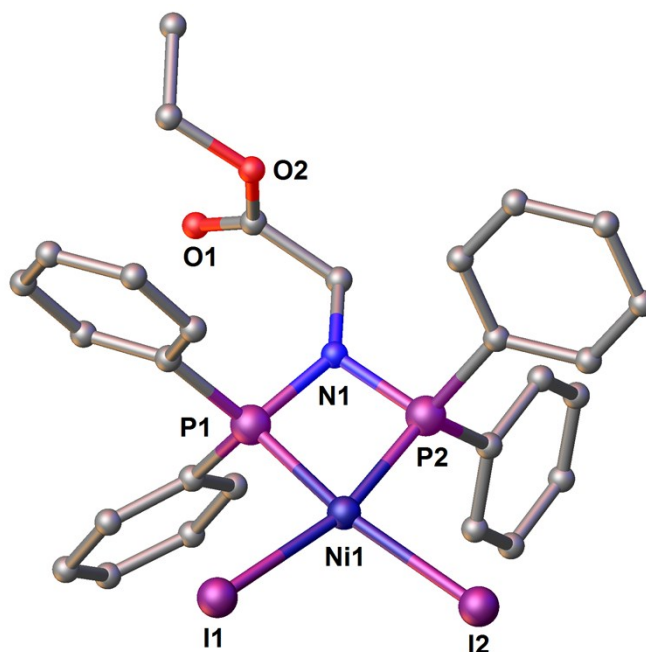


Fig. S8 Molecular structure of **4b**. Hydrogen atoms are omitted for clarity. Selected interatomic distances (Å) and angles (°) : Ni1–P1 2.1366(8), Ni1–P2 2.1285(8), Ni1–I1 2.5150(5), Ni1–I2 2.5094(5), P1–N1 1.699(2), P2–N1 1.699(2); P1–Ni1–P2 74.00(3), P1–Ni1–I1 92.66(3), I1–Ni1–I2 100.178(18), P1–N1–P2 98.12(10).

4. IR and ^1H (^{31}P , ^{11}B , ^{19}F) NMR spectra of **5b**.

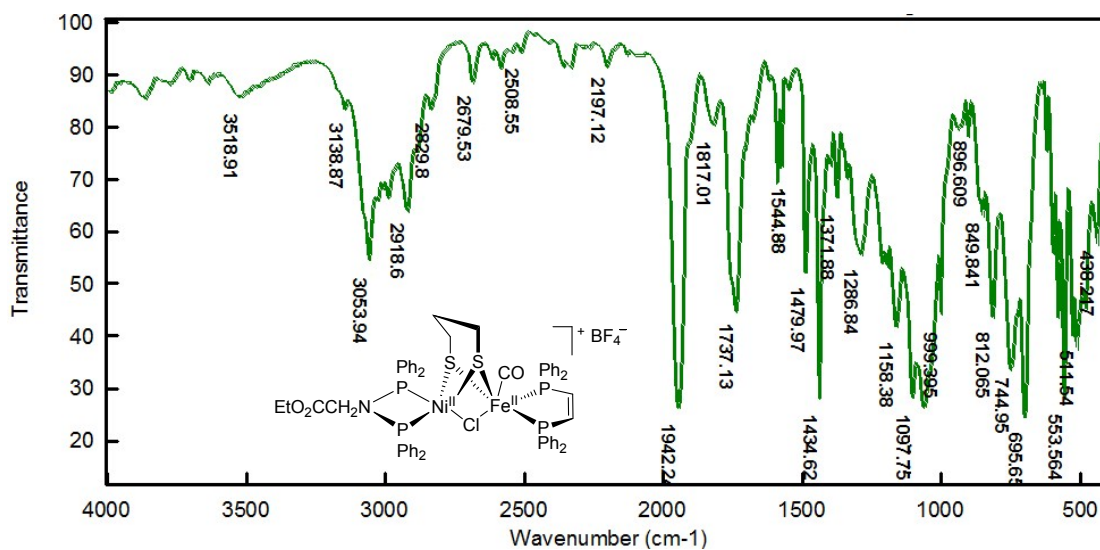


Fig. S9 IR spectrum of **5b**

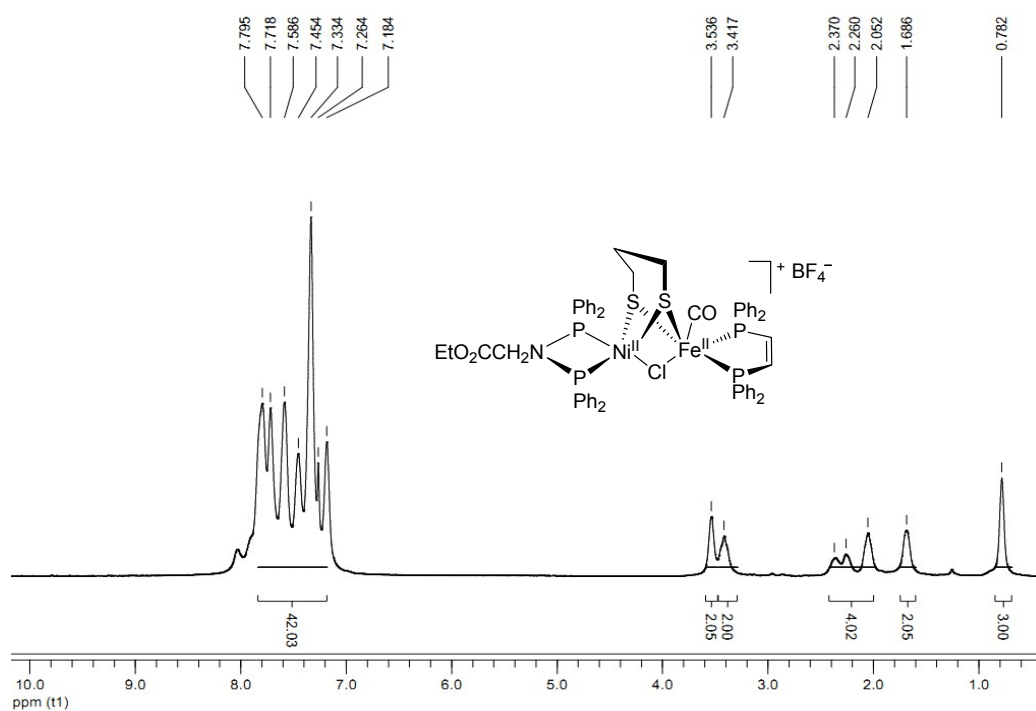


Fig. S10 ^1H NMR spectrum of **5b**.

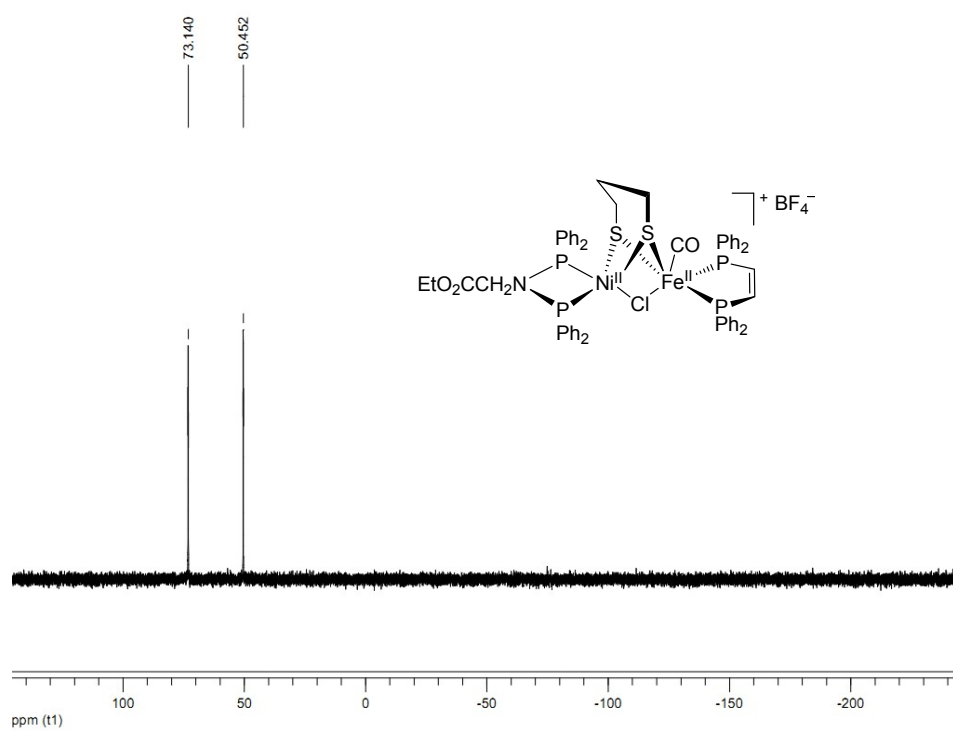


Fig. S11 ³¹P NMR spectrum of **5b**.

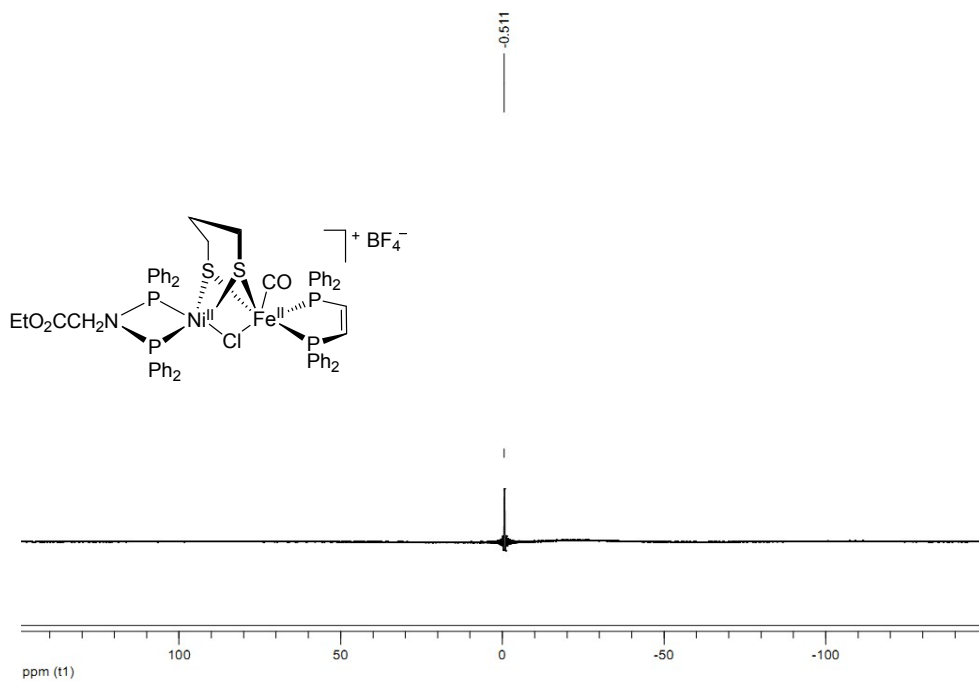


Fig. S12 ¹¹B NMR spectrum of **5b**.

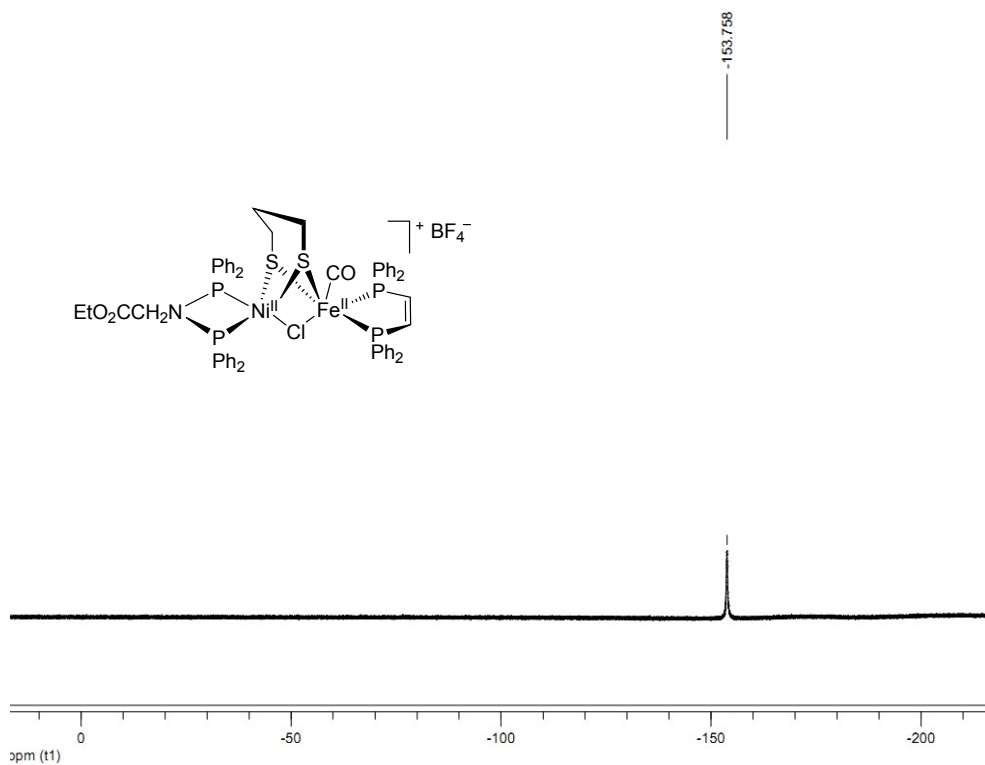


Fig. S13 ^{19}F NMR spectrum of **5b**.

5. IR and ^1H (^{31}P , ^{11}B , ^{19}F) NMR spectra of **6a**

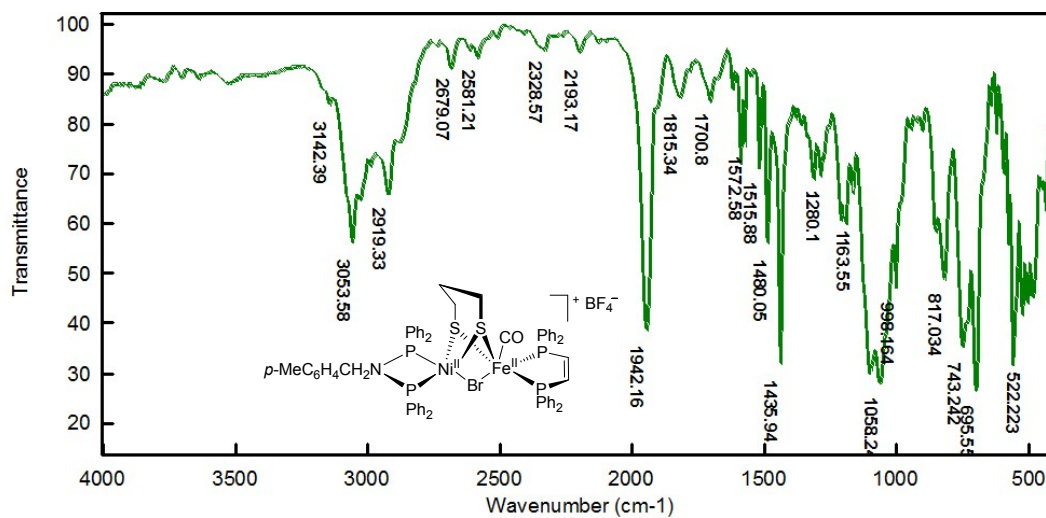


Fig. S14 IR spectrum of **6a**.

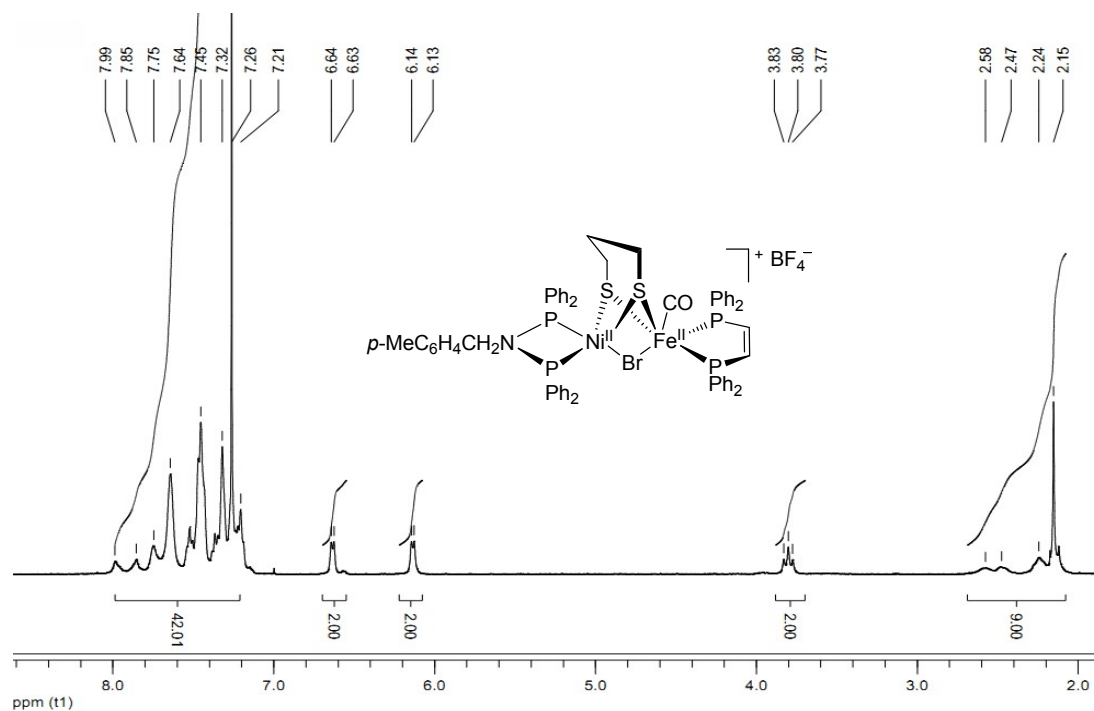


Fig. S15 ^1H NMR spectrum of **6a**.

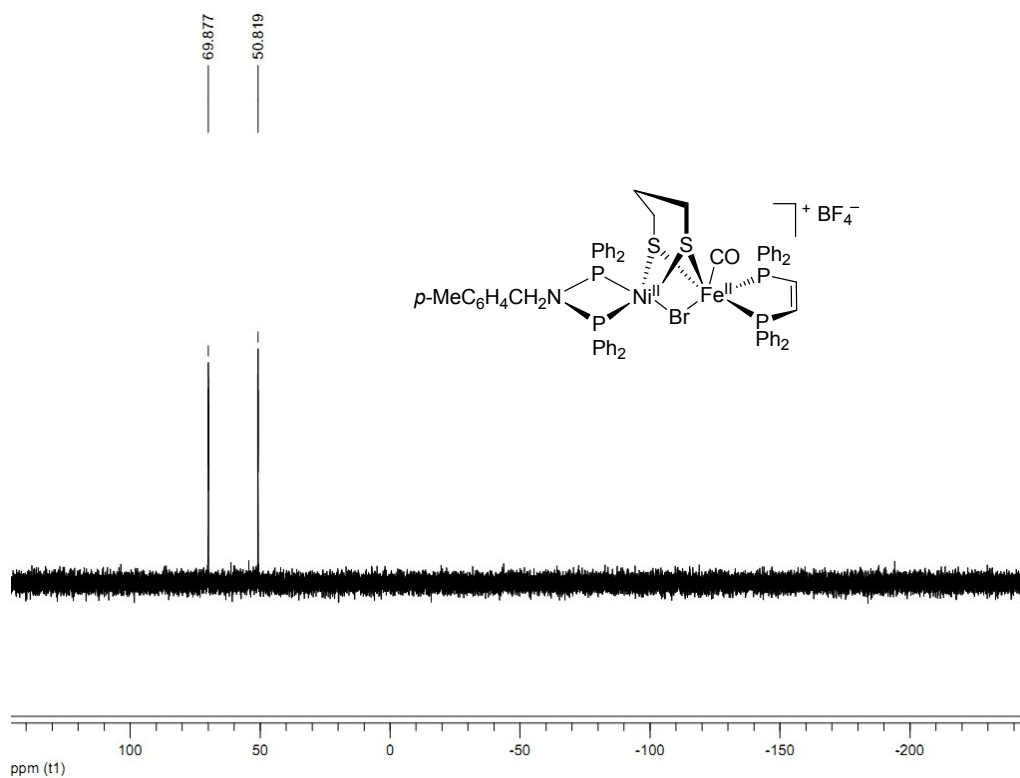


Fig. S16 ³¹P NMR spectrum of **6a**.

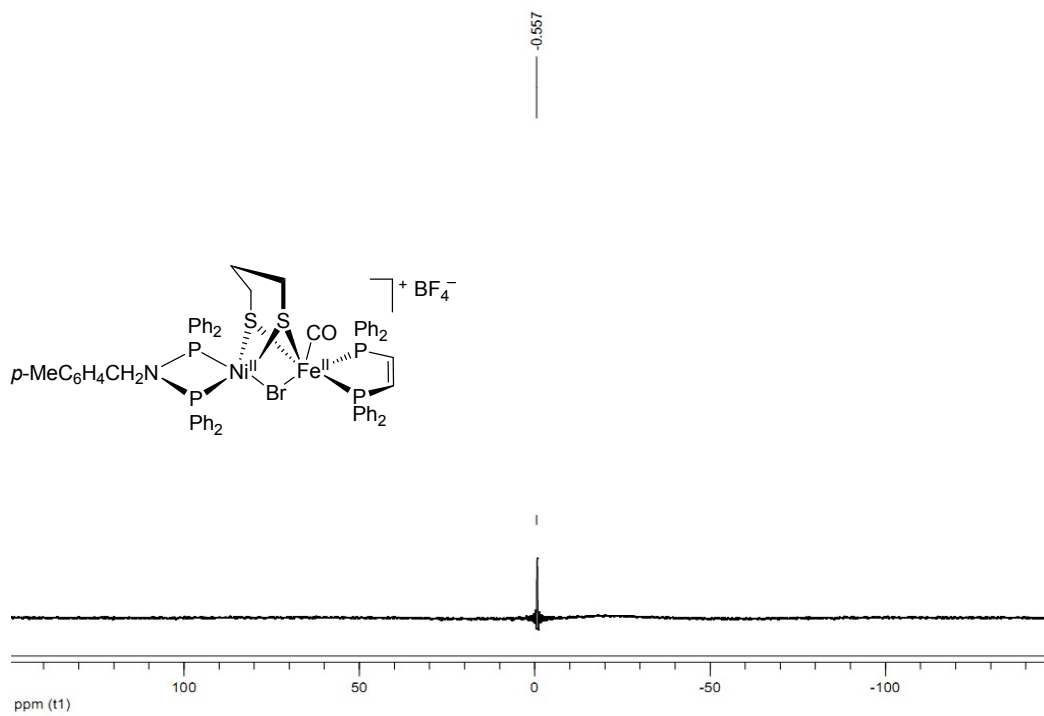


Fig. S17 ¹¹B NMR spectrum of **6a**.

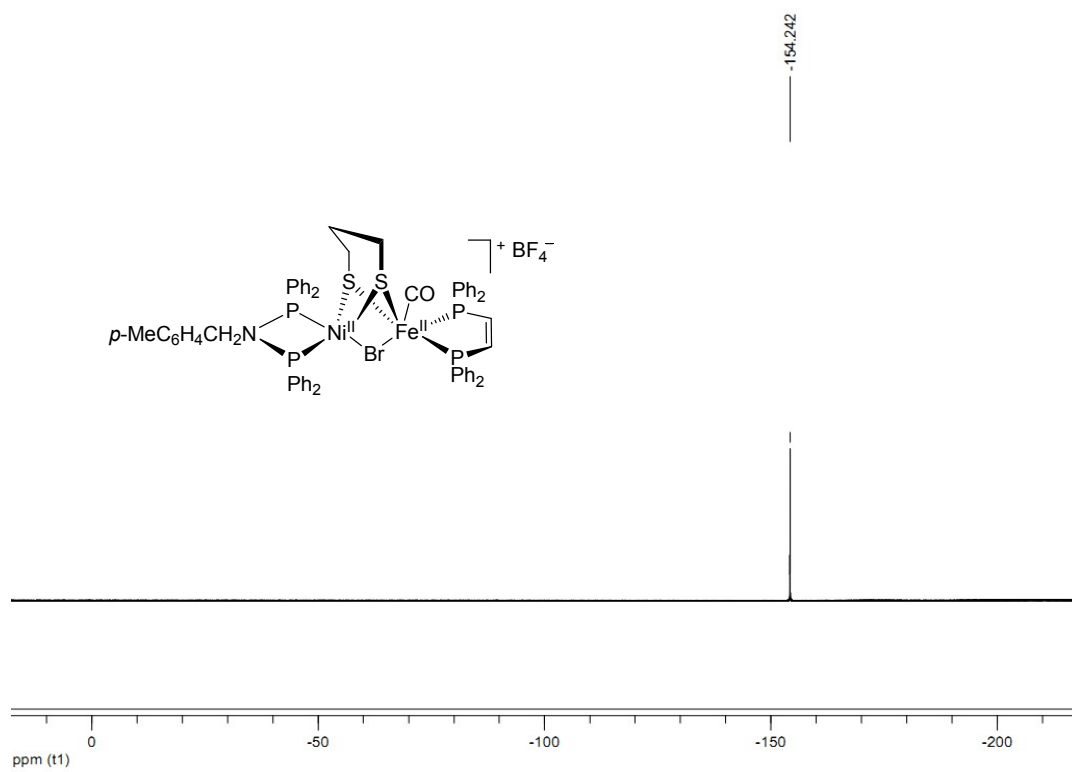


Fig. S18 ^{19}F NMR spectrum of **6a**.

6. IR and ^1H (^{31}P , ^{11}B , ^{19}F) NMR spectra of **7a**

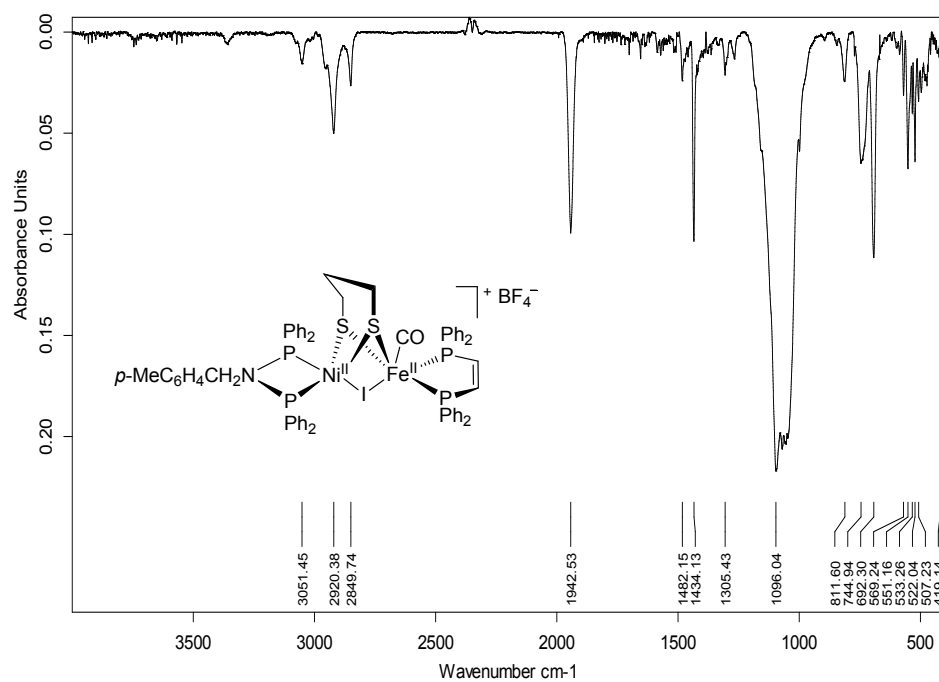


Fig. S19 IR spectrum of **7a**.

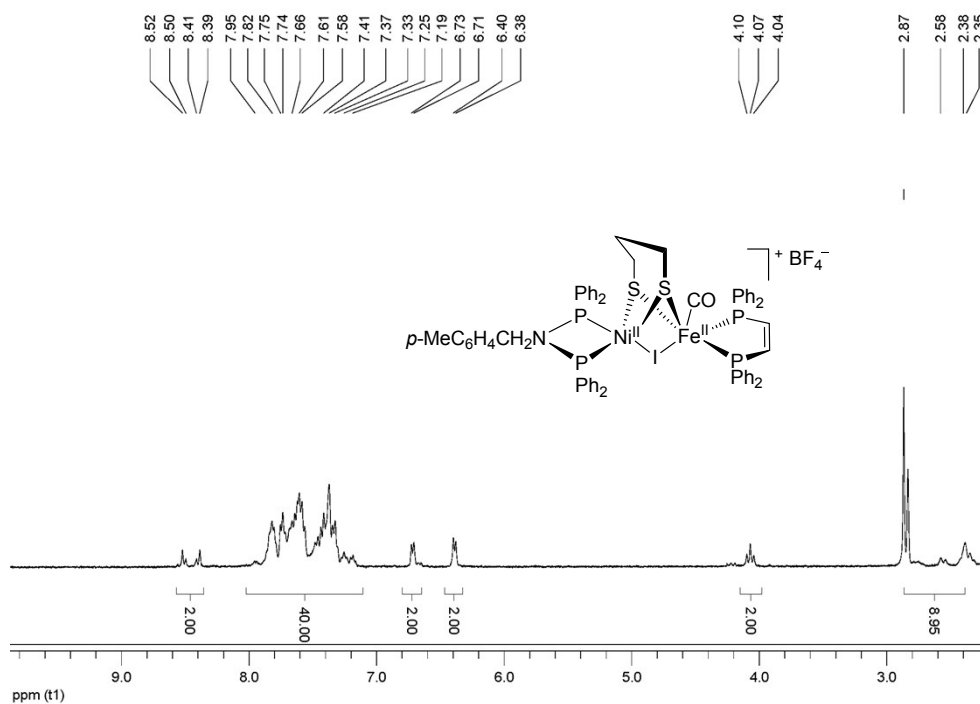


Fig. S20 ^1H NMR spectrum of **7a**.

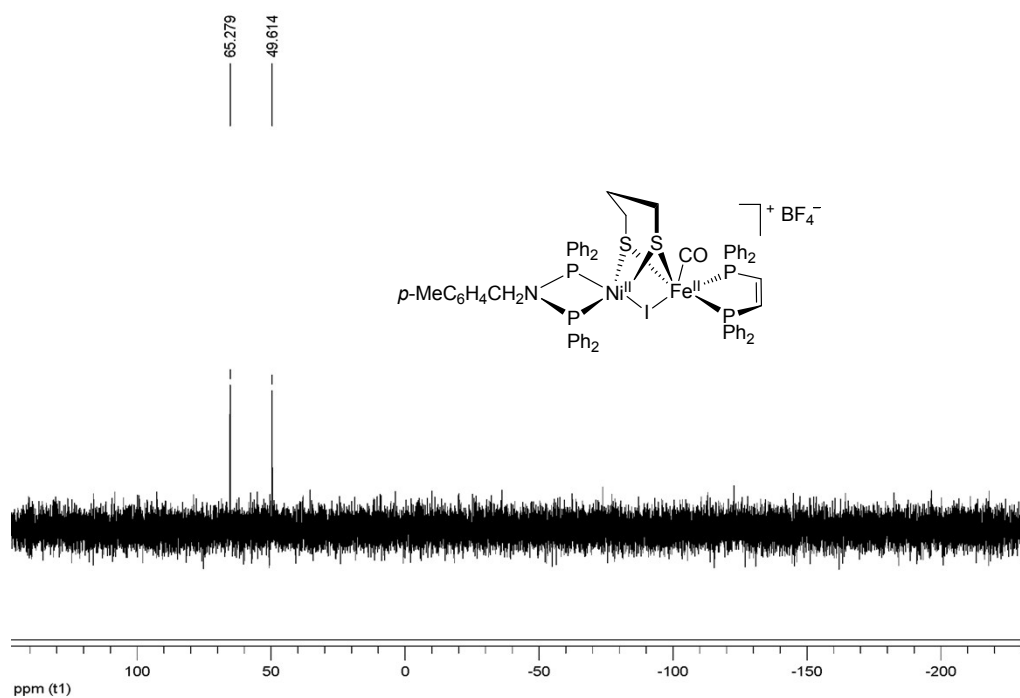


Fig. S21 ^{31}P NMR spectrum of **7a**.

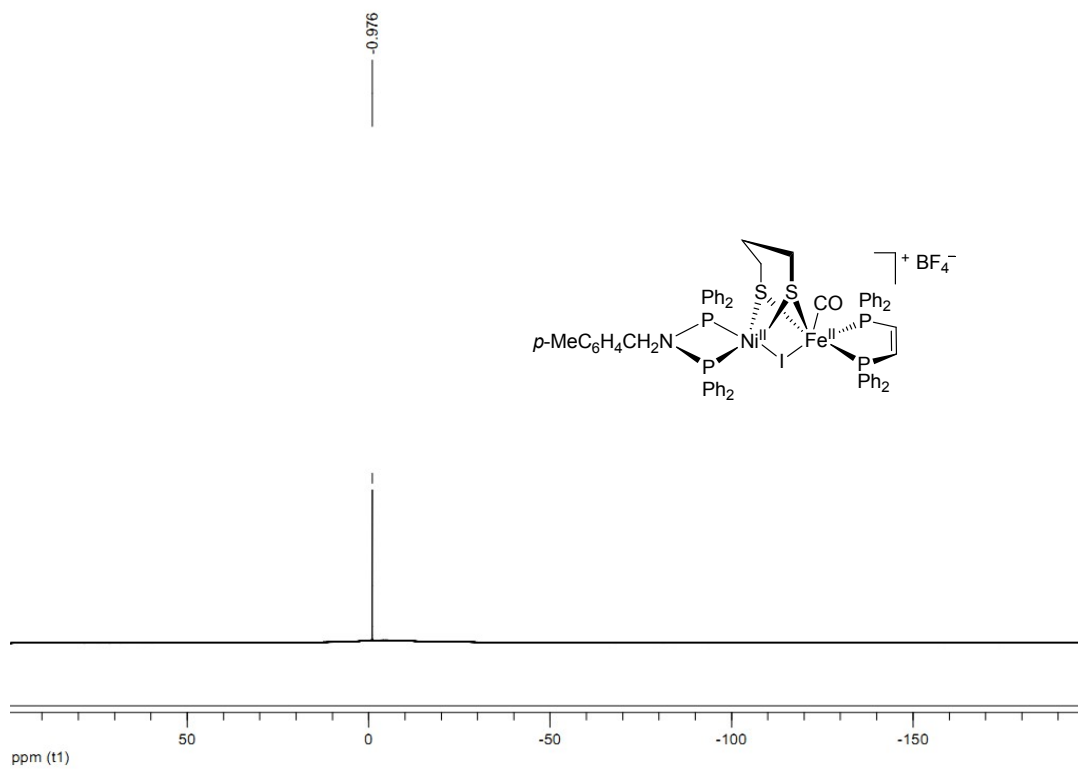


Fig. S22 ^{11}B NMR spectrum of **7a**.

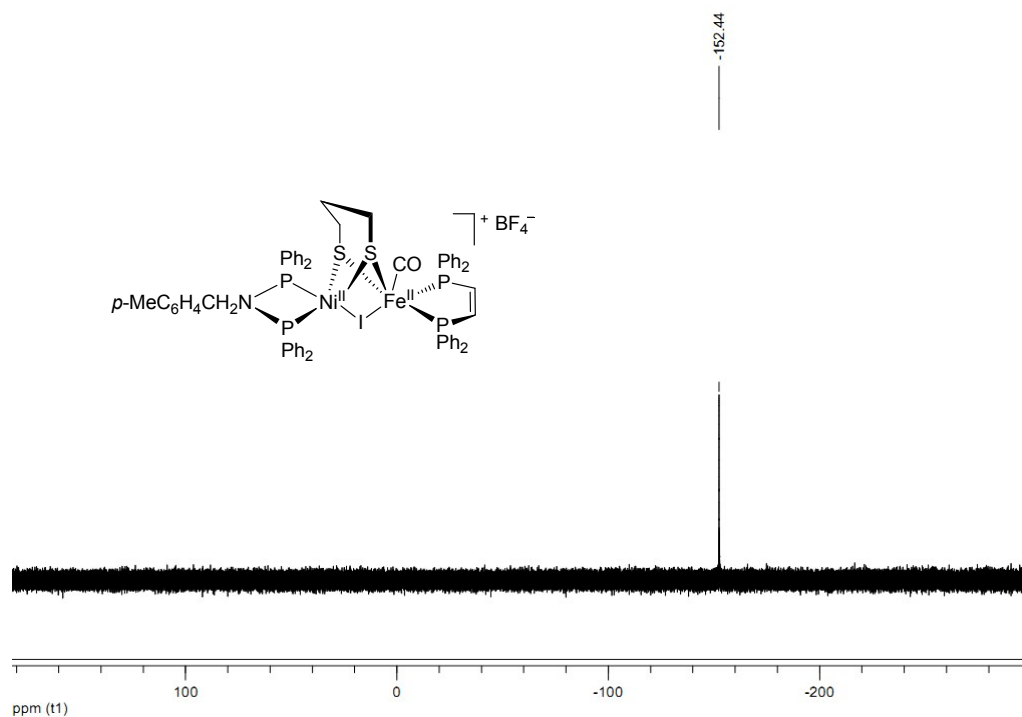


Fig. S23 ^{19}F NMR spectrum of **7a**.

7. Bulk electrolysis for the two-electron reduction of $[\text{CpFe}(\text{CO})_2]_2$ and the one-electron reductions of **5a–7a**.

The reduction events for **5a–7a** is a one-electron process since their final Q values determined by bulk electrolysis are close to half that of the known two-electron reduction process of dimer $[\text{CpFe}(\text{CO})_2]_2$.^{1,2}

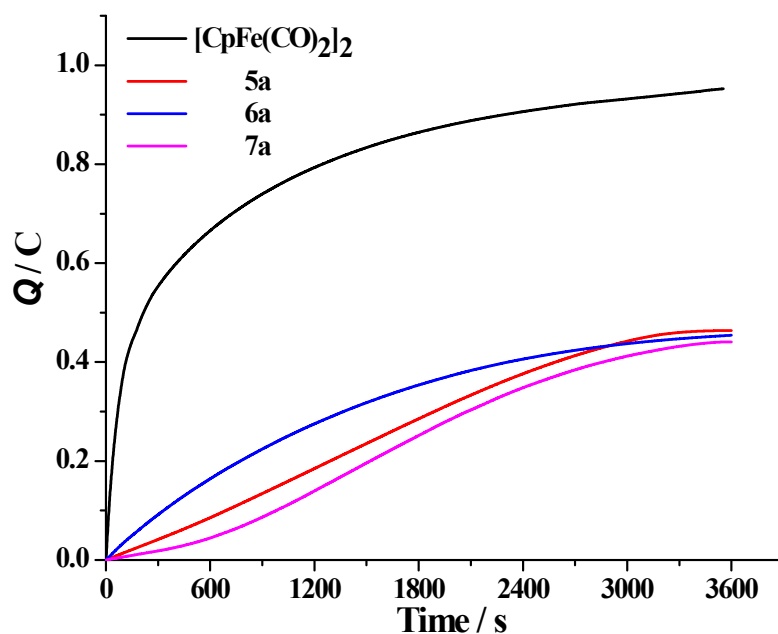


Fig. S24 Bulk electrolysis for the two-electron reduction of $[\text{CpFe}(\text{CO})_2]_2$ and the one-electron reductions of **5a–7a**.

8. Bulk electrolysis for the two-electron reduction of $[\text{CpFe}(\text{CO})_2]_2$ and the one-electron oxidations of **5a–7a**.

The oxidation events for **5a–7a** are also a one-electron process since the final Q values determined by bulk electrolysis are close to half that of the known two-electron reduction of dimer $[\text{CpFe}(\text{CO})_2]_2$.^{1,2}

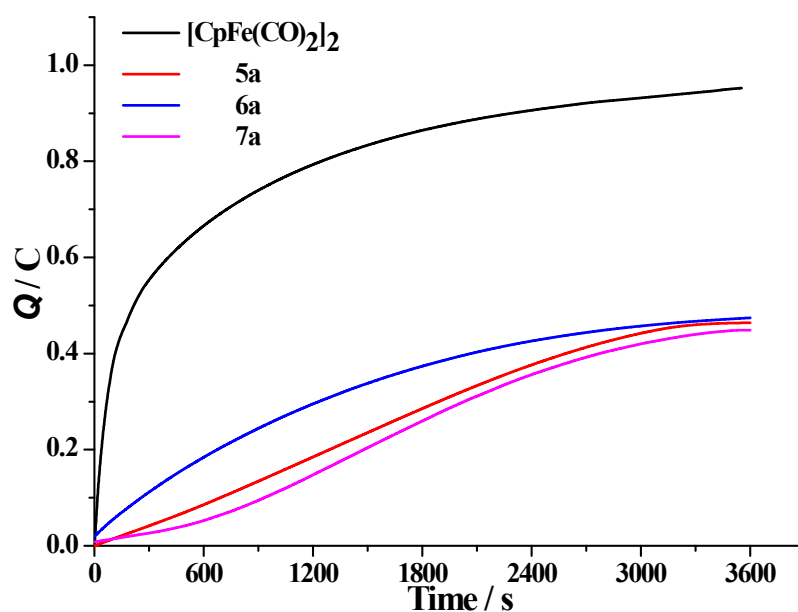


Fig. S25 Bulk electrolysis for the two-electron reduction of $[\text{CpFe}(\text{CO})_2]_2$ and the one-electron oxidations of **5a–7a**.

9. Plots of i_p versus $v^{1/2}$ for the reduction peaks of 5a–7a.

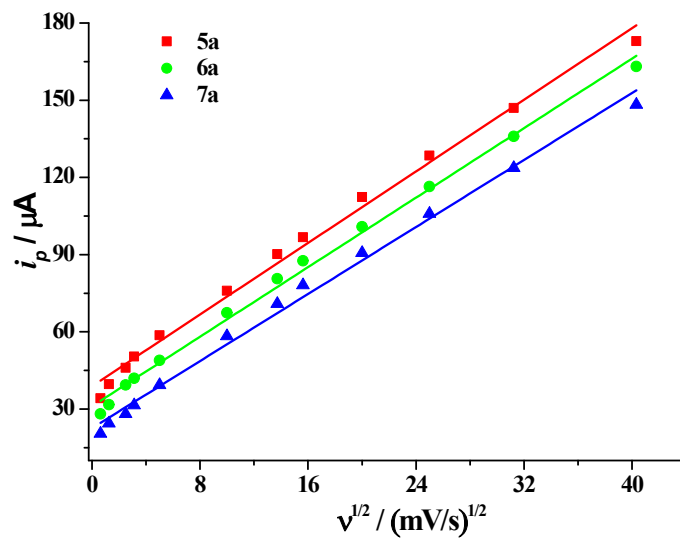


Fig. S26 Plots of i_p versus $v^{1/2}$ for the reduction peaks of 5a (■), 6a(●)and 7a(▲).

10. Cyclic voltammograms and overpotential determinations of 6a,b and 7a,b with Cl₂CHCO₂H in MeCN.

Since the pK_a and the standard redox potential of Cl₂CHCO₂H in MeCN ($pK_a^{\text{MeCN}} = 13.2$, $E_{\text{H}^+/\text{H}_2}^0 = -0.14 \text{ V}$)³ are known, the equilibrium potential ($E_{\text{HA}}^0 = -0.92 \text{ V vs Fc/Fc}^+$) can be calculated according to eq.S1 using Evans' relationship.³ The overpotentials of the electrocatalytic proton reductions catalyzed by **6a,b** and **7a,b** were measured using eq.S2 from the potential at 0.5 (i_{pc}), where i_{pc} is the cathodic peak current in the cyclic voltammogram recorded after addition of 40 mM or 68 mM of Cl₂CHCO₂H.

$$E_{\text{HA}}^0 = E_{\text{H}^+/\text{H}_2}^0 - (2.303RT/F)pK_{a,\text{HA}} \quad \text{eq.S1}$$

$$\text{overpotential} = |E_{\text{HA}}^0 - E_{\text{cat}/2}| \quad \text{eq.S2}$$

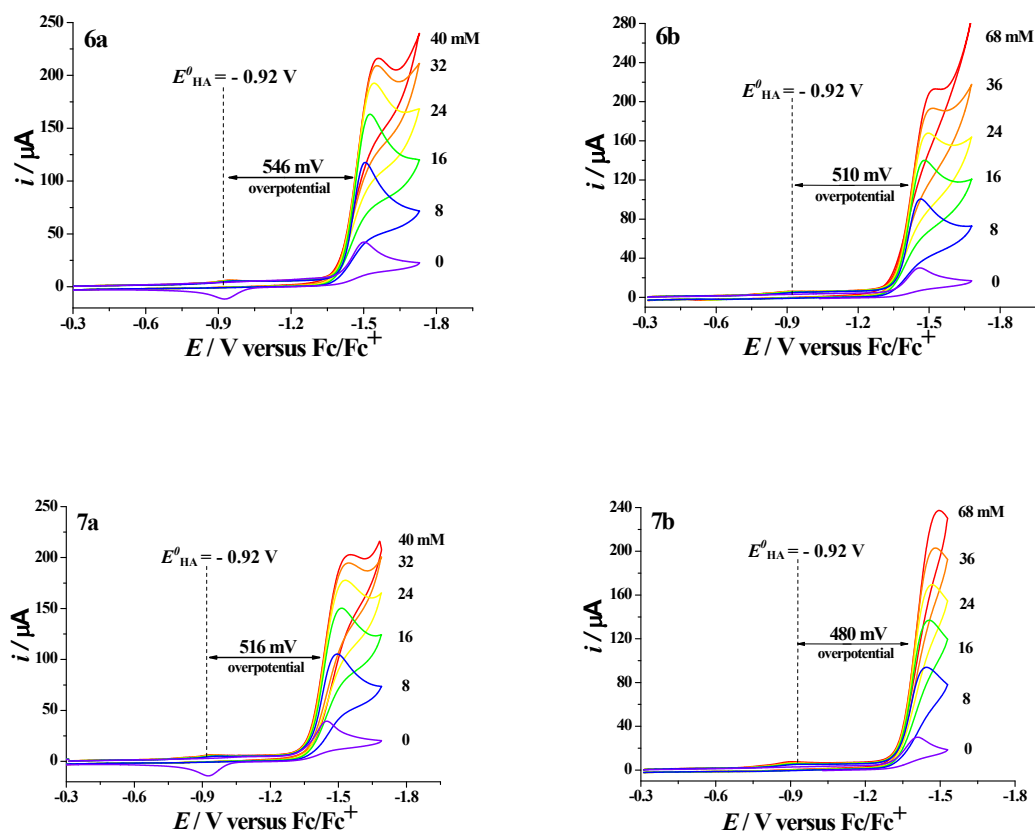


Fig. S27 Cyclic voltammograms of **6a,b** and **7a,b** (1.0 mM) with varying amount of Cl₂CHCO₂H (denoted on right) in 0.1 M *n*-Bu₄NPF₆/MeCN at a scan rate of 0.1 Vs⁻¹.

11. TOF calculations

The turnover frequency (TOF) was calculated using a ratio of i_{cat}/i_p (eqs. S3 and S4), where i_{cat} is the peak current of the reduction wave in the presence of acid and i_p is the peak current in the absence of acid. The value of i_{cat}/i_p is in the regime where the catalytic rate is independent of $[\text{H}]^+$.⁴

$$i_{\text{cat}}/i_p = (n/0.446)(RTk/Fv)^{1/2} \quad \text{eq. S3}$$

$$\text{TOF} = 1.94v(i_{\text{cat}}/i_p)^2 \quad \text{eq. S4}$$

n = number of electrons transferred R = ideal gas constant in $\text{K}^{-1}\text{mol}^{-1}$

T = temperature in K k = rate constant

v = scan rate in V/ s

$$\text{TOF}_{5a} = 1.94v(i_{\text{cat}}/i_p)^2 = 1.94 (\text{V}^{-1}) \times 0.1 (\text{Vs}^{-1}) \times (7.0)^2 = 9.5$$

$$\text{TOF}_{5b} = 1.94v(i_{\text{cat}}/i_p)^2 = 1.94 (\text{V}^{-1}) \times 0.1 (\text{Vs}^{-1}) \times (9.3)^2 = 16.8$$

$$\text{TOF}_{6a} = 1.94v(i_{\text{cat}}/i_p)^2 = 1.94 (\text{V}^{-1}) \times 0.1 (\text{Vs}^{-1}) \times (6.0)^2 = 7.0$$

$$\text{TOF}_{6b} = 1.94v(i_{\text{cat}}/i_p)^2 = 1.94 (\text{V}^{-1}) \times 0.1 (\text{Vs}^{-1}) \times (8.1)^2 = 12.7$$

$$\text{TOF}_{7a} = 1.94v(i_{\text{cat}}/i_p)^2 = 1.94 (\text{V}^{-1}) \times 0.1 (\text{Vs}^{-1}) \times (5.4)^2 = 5.7$$

$$\text{TOF}_{7b} = 1.94v(i_{\text{cat}}/i_p)^2 = 1.94 (\text{V}^{-1}) \times 0.1 (\text{Vs}^{-1}) \times (7.9)^2 = 12.1$$

12. References

- 1 L.-C. Song, B. Gai, Z.-H. Feng, Z.-Q. Du, Z.-J. Xie, X.-J. Sun and H.-B. Song, *Organometallics*, 2013, **32**, 3673-3684.
- 2 L.-C. Song, Y.-X. Wang, X.-K. Xing, S.-D. Ding, L.-D. Zhang, X.-Y. Wang and H.-T. Zhang, *Chem. Eur. J.*, 2016, **22**, 16304-16314.
- 3 G. A. N. Felton, R. S. Glass, D. L. Lichtenberger and D. H. Evans, *Inorg. Chem.*, 2006, **45**, 9181-9184.
- 4 M. E. Carroll, B. E. Barton, D. L. Gray, A. E. Mack and T. B. Rauchfuss, *Inorg. Chem.*, 2011, **50**, 9554-9563.